PHYSICAL REVIEW B VOLUME 41, NUMBER 4 1 FEBRUARY 1990

Oscillations of a fluxon in a finite-length ac-biased Josephson junction

Boris A. Malomed
P. P. Shirshov Institute for Oceanology, U.S.S.R. Academy of Sciences, 23 Krasikov Street, Moscow, 117218, U.S.S.R.
(Received 19 June 1989)

A model of a moderate-length damped Josephson junction with an ac drive applied at its edges is considered, and a uniformly distributed dc drive is also taken into account. Dynamics of a fluxon oscillating between the edges are reduced to a discrete map. It is demonstrated analytically that, with the increase of the ac-drive's amplitude, a solution appears that describes periodic oscillations of the fluxon; with the subsequent growth of the amplitude, this solution undergoes a period-doubling bifurcation that is demonstrated to be supercritical. These analytical results are in accordance with recent numerical findings reported by Salerno *et al.*

Fluxon oscillations in a long but finite Josephson junction are a traditional object of theoretical studies (see, e.g., Ref. 1). A long dc-biased damped Josephson junction is described by the well-known model of McLaughlin and Scott[2]

$$\phi_{tt}-\phi_{xx}+\sin\phi=-\alpha\phi_t-\tfrac{1}{2}f \ , \tag{1}$$

where ϕ is the normalized magnetic flux in the junction, α is a phenomenological dissipation constant, and f is the dc bias current density (external drive for fluxons). An ac component of the drive can be generated by external rf field applied to the junction. The corresponding boundary conditions[3] at the junction's edges $x=0$ and L are given, in a general case, by a linear combination of the two following sets of equations:

$$\phi_x(x=0)=-\tfrac{1}{2}\epsilon\sin(\omega t) \ , \quad \phi_x(x=L)=-\tfrac{1}{2}\epsilon\sin(\omega t) \ , \tag{2a}$$

$$\phi_x(x=0)=-\tfrac{1}{2}\epsilon\sin(\omega t) \ , \quad \phi_x(x=L)=+\tfrac{1}{2}\epsilon\sin(\omega t) \ . \tag{2b}$$

Following Ref. 4, I will refer to the couplings of the rf field to the junction corresponding to the boundary conditions (2a) and (2b) as to the magnetic and electric couplings, respectively.

A fluxon is described by the exact solution to the unperturbed equation (1) (i.e., the one with $\alpha=f=0$)

$$\phi_k(x,t)=4\tan^{-1}(\exp\{\sigma[x-\xi(t)](1-V^2)^{-1/2}\}) \ , \tag{3}$$

where $\sigma=\pm1$, $\xi(t)=Vt$, and V are, respectively, the fluxon's polarity, center-of-mass coordinate, and velocity. If the junction is sufficiently long ($L\gg1$), a fluxon near an edge is described (in the case $\epsilon=0$) by the so-called breather solution (see, e.g., Ref. 5). We are interested in the low-frequency breather which has the approximate form

$$\phi_{br}=4\tan^{-1}[\zeta^{-1}\sin(\zeta t)\operatorname{sech}x], \quad |\zeta|\ll1 \tag{4}$$

[of course, the solution (4) is physically meaningful only at $x>0$]. The breather (4) may be interpreted as a bound state of a fluxon in the physical region $x\geq0$ and its "mirror image" (antifluxon) in the unphysical region $x<0$, the distance between them being

$$2l\approx\ln[4\zeta^{-2}\sin^2(\zeta t)] \ , \tag{5}$$

provided $e^{-2l}\ll1$. As it follows from Eq. (5), the time between a maximum overlapping of the fluxon with the edge [$t=0$ in Eq. (5)] and a moment when the fluxon is at the middle of the junction ($l=L/2$) is

$$\tfrac{1}{2}\tau=\zeta^{-1}\sin^{-1}(\tfrac{1}{2}\zeta e^{L/2}) \ . \tag{6}$$

The solution (4) and the relations (5) and (6) are meaningful both for real and imaginary ζ: In the latter case, the solution (4) describes a free fluxon-antifluxon pair.

The energy of the fluxon described by the expression (4) at $x\geq0$ is

$$E_k\approx8-4\zeta^2 \tag{7}$$

(including the case of imaginary ζ). As it has been demonstrated in Ref. 6, a reflection of the fluxon from the edge $x=0$ (at $\epsilon\neq0$) gives rise to the change

$$\Delta_1E=-4\pi\epsilon e^{-\omega}\sin\delta_n, \quad \delta_n\equiv\omega t_n \ , \tag{8}$$

of the kink's energy, t_n being the reflection moment. The dissipation [$\alpha\neq0$ in Eq. (1)] gives rise to the additional item[1,4,6]

$$\Delta_2E=-4\pi^2\alpha+O(\alpha\zeta) \ . \tag{9}$$

At last, a flight of the fluxon between the edges of the junction gives rise to the energy input

$$\Delta_3E=-\pi\sigma fL \tag{10}$$

from the dc drive.

As it follows from Eqs. (6)–(10), the dynamics of the fluxon reduce to the discrete map (similar to the ones obtained for allied problems in Ref. 6), which takes the form

$$\zeta_{n+1}^2=\zeta_n^2+\pi(\pi\alpha+\tfrac{1}{4}\sigma fL)+\pi\epsilon\sin\delta_n\ ,$$
$$\delta_{n+1}=\delta_n+\pi+2\omega\zeta_{n+1}^{-1}\sin^{-1}(\tfrac{1}{2}\zeta_{n+1}e^{L/2}) \tag{11a}$$

in the case of the magnetic coupling, and

$$\zeta_{n+1}^2=\zeta_n^2+\pi(\pi\alpha+\tfrac{1}{4}\sigma fL)+\pi\epsilon\sin\delta_n\ ,$$
$$\delta_{n+1}=\delta_n+2\omega_{n+1}^{-1}\sin^{-1}(\tfrac{1}{2}\zeta_{n+1}e^{L/2}) \tag{11b}$$

in the case of the electric coupling. In Eqs. (11), the index n refers to nth reflection of the fluxon from *either* edge $x=0$ or $x=L$, and it is implied $\omega \ll 1$ (the low frequencies ω will be of basic interest below).

The map (11a) has stationary points with the coordinates (ζ_0, δ_0), where

$$\sin\delta_0=-\epsilon^{-1}(\pi\alpha+\tfrac{1}{4}\sigma fL)\ , \tag{12}$$

and ζ_0 is determined by the transcendental equation

$$2\zeta_0^{-1}\sin^{-1}(\tfrac{1}{2}\zeta_0 e^{L/2})=(2m-1)\pi/\omega\ ,\quad m=1,2,3,\ldots\ . \tag{13}$$

For the map (11b), the multiplier $(2m-1)$ in Eq. (13) must be replaced by $2m$. Equation (13) remains valid for imaginary ζ too: In this case it takes the form

$$2|\zeta_0|^{-1}\ln[\tfrac{1}{2}|\zeta_0|e^{L/2}+(1+\tfrac{1}{4}|\zeta_0|^2e^L)^{1/2}]=(2m-1)\pi/\omega\ . \tag{14}$$

A schematic graph of the function

$$g(\zeta_0)\equiv 2\zeta_0^{-1}\sin^{-1}(\tfrac{1}{2}\zeta_0 e^{L/2})$$

for ζ_0 both real and imaginary is shown in Fig. 1. The values marked in Fig. 1 are

$$\zeta_{\max}^2=4e^{-L};\quad g_{\max}=\frac{\pi}{2}e^{L/2};\quad g_0=e^{L/2}\ . \tag{15}$$

As it follows from Eq. (12), the stationary point exists if ϵ^2 exceeds the threshold value

$$\epsilon_0^2=(\pi\alpha+\tfrac{1}{4}\sigma fL)^2\ ; \tag{16}$$

note that ϵ_0^2 depends on the fluxon's polarity σ. Less trivial is the fact that there is also a frequency threshold. Indeed, it follows from Eqs. (13)–(15) that a solution exists provided

$$\omega \ge \omega_{\min}\equiv 2e^{-L/2}\ , \tag{17}$$

which corresponds to $m=1$ in Eq. (13); in the case of the electric coupling $\omega_{\min}=4e^{-L/2}$.

To investigate the stability of the stationary point, let us linearize the maps (11) in its vicinity:

$$\zeta_n=\zeta_0+\tilde{\zeta}_n,\quad \delta_n=\delta_0+\tilde{\delta}_n\ . \tag{18}$$

Insertion of Eq. (18) into the linearized Eqs. (11) yields the following equation for the multiplicators λ defined by the relations $\tilde{\zeta}_{n+1}=\lambda\tilde{\zeta}_n$, $\tilde{\delta}_{n+1}=\lambda\tilde{\delta}_n$:

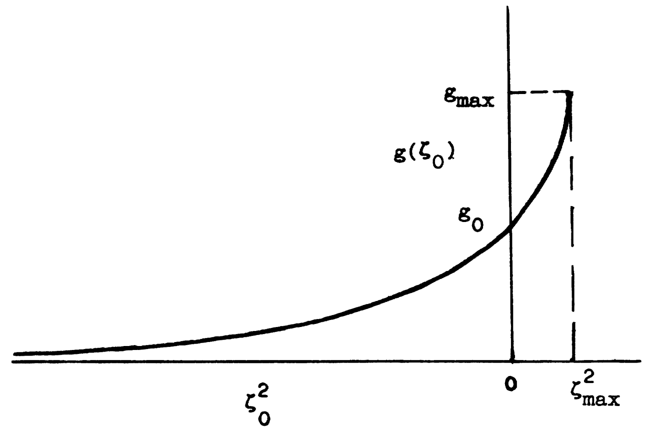

FIG. 1. A schematic graph of the function $g(\zeta_0)$ for both signs of ζ_0^2.

$$(\lambda-1)^2-\mu(\lambda-1)-\mu=0\ , \tag{19}$$

where

$$\mu\equiv\frac{\pi\epsilon\omega\cos\delta_0}{2\zeta_0^3}[e^{L/2}\zeta_0(1-\tfrac{1}{4}e^L\zeta_0^2)^{-1/2}-2\sin^{-1}(\tfrac{1}{2}e^{L/2}\zeta_0)]\ . \tag{20}$$

As it follows from Eq. (19), the stability condition $|\lambda|<1$ takes the form

$$-4\le\mu\le 0\ . \tag{21}$$

Note that Eq. (12) determines only $|\cos\delta_0|$, while the sign of $\cos\delta_0$ remains arbitrary. It can be demonstrated that the expression in the square brackets of Eq. (20) is always positive. So, Eqs. (20) and (21) tell us that stable is the stationary point for which $\epsilon\cos\delta_0<0$.

To analyze change of stability of the stationary point, let us follow the increase of ϵ^2 at fixed values of other parameters. As we have seen above, the stationary point (12),(13) appears at the value (16) of ϵ^2. Inserting the expression (20) into the stability condition (21), it is straightforward to find that the point becomes unstable at

$$\epsilon^2=\epsilon_1^2\equiv\epsilon_0^2+(8\zeta_0^3/\pi\omega)^2[e^{L/2}\zeta_0(1-\tfrac{1}{4}e^L\zeta_0^2)^{-1/2}-2\sin^{-1}(\tfrac{1}{2}e^{L/2}\zeta_0)]^{-2}\ , \tag{22}$$

when $\mu=-4$ [see Eq. (20)].

According to Eq. (19), $\lambda=-1$ at $\mu=-4$. This circumstance implies that at $\epsilon^2=\epsilon_1^2$ the stationary point becomes unstable against period-doubling perturbations. To analyze the bifurcation, i.e., to find out which new stable solutions appear, it is necessary to take account of nonlinear terms in the expansions of the maps (11) near the stationary point (12),(13). This can be done explicitly in the case when ω is close to the threshold value (17) or to its multiple.

Let us set (for the magnetic coupling)

$$\omega=(2m-1)2e^{-L/2}+\Omega,\quad 0<\Omega\ll e^{-L/2}\ . \tag{23}$$

In this case, ζ will be close to the value $\zeta_{\max}$ [see Eqs. (15)], so it is convenient to introduce the new quantity

$$z_n^2 \equiv 2e^{-L/2} - \zeta_n, \quad 0 < z_n^2 \ll e^{-L/2} . \tag{24}$$

At last, let us define

$$\Psi_n \equiv \delta_n - (2\pi m)n , \tag{25}$$

m being the same integer as in Eq. (23). Inserting Eqs. (23)–(25) into Eqs. (11a) brings us to the map

$$z_{n+1}^2 = z_n^2 - \frac{\pi}{4} e^{L/2}(\pi\alpha + \tfrac{1}{2}\sigma f L) - \frac{\pi}{4}\epsilon e^{L/2}\sin\Psi_n ,$$
$$\Psi_{n+1} = \Psi_n + \frac{\pi}{2} e^{L/2}\Omega - 2(2m-1)e^{L/4} z_{n+1} . \tag{26}$$

In terms of this map, the stationary point (12),(13) takes the form

$$\sin\Psi_0 = -\epsilon^{-1}(\pi\alpha + \tfrac{1}{2}\sigma f L) ,$$
$$z_0 = \frac{\pi}{4}(2m-1)^{-1}\Omega e^{L/4} , \tag{27}$$

and the stability condition (21) takes the form

$$-4 \le (2m-1)^2 \Omega^{-1} e^{L/2} \epsilon \cos\Psi_0 \le 0 .$$

At last, the final stability condition (22) reduces to the following one:

$$\epsilon^2 < \epsilon_1^2 \equiv \epsilon_0^2 + (2m-1)^{-4}(4\Omega)^2 e^{-L} . \tag{28}$$

The stationary point (27) corresponds to periodic shuttle oscillations of the fluxon between the junction's edges, the oscillation period being 2τ [see Eq. (6)]. It is important that, in the state considered, the shuttle motions forth and back are fully symmetric. The period doubling means breakup of this symmetry. Let us look for solutions which describe the period doubling in the form

$$z_{n-1} = z_{n+1} \equiv z_0 + z_1, \quad z_n = z_{n+2} \equiv z_0 + z_2 ;$$
$$\Psi_{n-1} = \Psi_{n+1} \equiv \Psi_0 + \Psi_1, \quad \Psi_n = \Psi_{n+2} \equiv \Psi_0 + \Psi_2 . \tag{29}$$

Inserting the expressions (29) into Eqs. (26), one can readily exclude the quantities z_1 and z_2 to arrive at the system of two equations

$$\sin(\Psi_0+\Psi_1) + \sin(\Psi_0+\Psi_2) = -2\epsilon^{-1}(\pi\alpha + \tfrac{1}{r}\sigma f L) ,$$
$$\Psi_1 - \Psi_2 = -\tfrac{1}{4}(2m-1)^2\Omega^{-1}\epsilon e^{L/2}[\sin(\Psi_0+\Psi_1) - \sin(\Psi_0+\Psi_2)] . \tag{30}$$

Expanding Eqs. (30) in powers of small $\Psi_{1,2}$, we obtain, in the first three orders of the expansion, the following results: $\Psi_1 = -\Psi_2$, and

$$\Psi_1^2 = 6(2m-1)^{-2}\Omega e^{-L/2}(\epsilon^2-\epsilon_0^2)^{1/2}(\epsilon^2+2\epsilon_0^2)^{-1} \times [(2m-1)^2\Omega^{-1}e^{L/2}(\epsilon^2-\epsilon_0^2)^{1/2}+4] . \tag{31}$$

According to Eq. (28), the right-hand side of Eq. (31) is negative and positive in the ranges where the stationary point (27) is, respectively, stable and unstable.

In the case of the electric coupling, setting $\omega = (2m)2e^{-L/2} + \Omega$ [cf. Eq. (23)], one can readily obtain the same final results (27) and (31) with $(2m-1)$ substituted by $2m$.

So, at $\epsilon^2 = \epsilon_1^2$ we encounter a typical fork-like bifurcation, and, at least in the limit case (23) (and in the analogous limit case for the electric coupling), this bifurcation is always *supercritical,* i.e., it gives rise to two new stable branches when the underlying one becomes unstable. The sequence of the two bifurcations considered (the ones at $\epsilon^2 = \epsilon_0^2$ and at $\epsilon^2 = \epsilon_1^2$) is illustrated by the diagram shown in Fig. 2. It is natural to expect that the period-doubling bifurcation at $\epsilon^2 = \epsilon_1^2$ is a first one in an infinite chain of period doublings which ends at a finite value of ϵ^2. This has been observed indeed in the recent work,[7] where a model of the fluxon shuttle based on a map which is a slight generalization of the one (11) was studied numerically. In Ref. 7, the bifurcation at $\epsilon^2 = \epsilon_1^2$ was treated only numerically, in contrast with the analytical treatment developed in the present work. A whole tree of the period-doubling bifurcations stemming from the sprout shown in Fig. 2 has been constructed in Ref. 7. In particular, the first period-doubling bifurcation observed in Ref. 7 is always supercritical, in accordance with the results reported here. In the same time, some branches of the bifurcation tree terminate at *subcritical* (inverted) higher bifurcations.

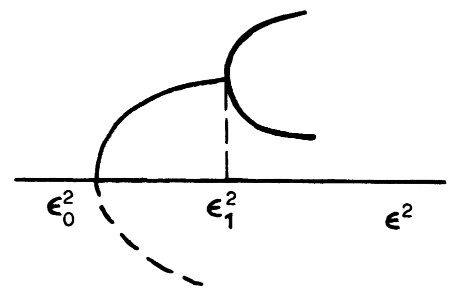

FIG. 2. The diagram of the bifurcations considered: At $\epsilon^2 = \epsilon_0^2$ two stationary points (12),(13) appear, the stable one being that for which $\epsilon\cos\delta_0 < 0$; at $\epsilon^2 = \epsilon_1^2$ the fork-like bifurcation takes place. The solid and dashed lines depict stable and unstable solutions, respectively.

In conclusion, it seems relevant to briefly discuss a difference between the analytical approach adopted in the present work and that developed for a similar problem (the so-called reverse ac Josephson effect) in Ref. 4. In the present paper, the analysis was based upon the fluxon's law of motion (5) supplemented by the energy balance equation ensuing from Eqs. (8)–(10). The law of motion (5) implies that a force of interaction of the fluxon with an edge $x=0$ or $x=L$, i.e., a force $\sim e^{-2x}$ or $\sim e^{-2(L-x)}$ (see Ref. 8) of attraction of the fluxon to its "mirror image" in the unphysical region $x<0$ or $x>L$, is dominating. It is easy to demonstrate that this force is indeed much greater than the friction force[2] $F_{fr} = -8\alpha V$ (V is the fluxon's velocity) corresponding to the law of motion (5). In the same time, we need to assume

$$e^{-L} \gtrsim f \tag{32}$$

to neglect the dc driving force[2] $F_{dr} = 2\sigma\pi f$ acting upon the fluxon. If the junction is very long, so that the inequality (23) does not hold, one may assume that the fluxon moves with the equilibrium velocity[2] V_0 determined by the equation $F_{dr}+F_{fr}=0$,

$$V_0^2(1-V_0^2)^{-1}=(\pi f/4\alpha)^2 . \tag{33}$$

The analysis developed in Ref. 4 was based on Eq. (33). As concerns the energy balance, the dissipative energy loss (9), generated by the reflection of the fluxon from a junction's edge, was neglected in Ref. 4.

ACKNOWLEDGMENTS

I am indebted to Mogens R. Samuelsen for useful discussions concerning the comparison between the results of the present work and those of Ref. 7.

[1]O. H. Olsen, N. F. Pedersen, M. R. Samuelson, H. Svensmark, and D. Welner, Phys. Rev. B **33**, 168 (1986).

[2]D. W. McLaughlin and A. C. Scott, Phys. Rev. A **18**, 1652 (1978).

[3]C. S. Owen and D. J. Scalapino, Phys. Rev. **164**, 538 (1967).

[4]J.-J. Chang, Phys. Rev. B **34**, 6137 (1986); **38**, 5081 (1988).

[5]O. H. Olsen and M. R. Samuelsen, Phys. Rev. B **34**, 3510 (1986).

[6]B. A. Malomed, Phys. Lett. A **123**, 494 (1987); Physica D **27**, 113 (1987).

[7]M. Salerno, M. R. Samuelsen, G. Filatrella, S. Pagano, and R. D. Parmentier, Phys. Rev. B (to be published); Phys. Lett. A **137**, 75 (1989).

[8]J. Rubinstein, J. Math. Phys. **11**, 258 (1970).